

Multi-Cell Full-Duplex Wireless Communication for Dense Urban Deployment

M. Moshiur Rahman

Dept. of Electrical Engineering

ETS, University of Quebec, Canada

mohammad-moshiur.rahman.1@ens.etsmtl.ca

Charles Despins

Dept. of Electrical Engineering

ETS, University of Quebec, Canada

charles.despins@etsmtl.ca

Aaron Callard, Gamini Senarath

Huawei Canada Research Center

aaron.callard@huawei.com, gamini.senarath@huawei.com

Sofiène Affes

INRS-EMT

University of Quebec, Canada

affes@emt.inrs.ca

Abstract—Simultaneous bidirectional transmission and reception of signals on a single channel in a full duplex (FD) system is gaining increased attention from both academia and industry. Recent advances in radio transceiver design have been able to minimize the self interference (SI) to a great extent making realization of a FD transceiver possible. For FD deployment in a multi-cell environment, minimizing SI is not sufficient due to the presence of a complex array of network-wide interference. This paper investigates the critical deployment challenges for a dense urban FD multi-cell network and provides solutions for successful deployment of FD cellular networks. Extensive simulation results show that the proposed user selection and power control algorithms are able to increase the FD performance gain by more than 80% when compared to the traditional half duplex (HD) counterpart.

I. INTRODUCTION

Wireless network data traffic is increasing in an exponential manner. This can be largely attributed to the growing number of smart phones, mobile computing devices, e.g., tablets, laptops, etc. The surging popularity of video content delivery services is further accelerating the increase in wireless data traffic. Cellular data traffic is predicted to increase by as much as 11 fold during the time period from 2013 to 2018 [1]. With the already existing spectrum scarcity problem, the need for a transmission solution with improved and sustainable spectrum efficiency is greater than ever before. Full duplex (FD) wireless systems can solve this problem to a great extent by using the same frequency channel simultaneously for both uplink (UL) and downlink (DL) transmissions. This can effectively almost double the radio link capacity.

In current systems, a radio transceiver typically operates in half duplex (HD) mode, i.e., it either transmits or receives at any particular time epoch or frequency. Radio transmission is done either using time division duplex (TDD) or frequency division duplex (FDD) mode where transmission (Tx) and reception (Rx) take place at separate time slots or frequencies. In this paper, we have investigated the TDD mode of operation and we will use the terms HD and TDD interchangeably. On the contrary, in a FD system, transmission and reception take

place at the same time. One of the main problems for FD communications is the interference from the transmitter to the receiver which is known as the self interference (SI). The SI is so high that it makes successful decoding of the received signal almost impossible. Hence, for successful realization of a FD system, the SI should be mitigated to such a level where decoding of received signal is possible [2].

In recent time, employing a combination analog and digital cancellation techniques, significant progress has been made to mitigate the SI. The SI cancellation using multiple antennas was studied in [3] and [4], where SI is cancelled by taking advantage of antenna position and directionality. Studies on single antenna systems [5], [6] show significant suppression of SI, where [6] has reported the ability to cancel SI by as much as 110 dB. Duarte *et al.* [7] have also reported to SI cancellation from 70 dB to 100 dB for multi antenna systems. To enable FD communication at the link-level, reducing SI is sufficient but for FD communication in a cellular level, measures must be taken to remove additional interference components.

Research in FD multi-cell systems is gaining momentum in recent time [8]. The DUPLO [9] project is investigating the FD system for small cell deployments; a joint UL-DL beamforming was designed for single cell deployment in [10]. In [11], a scheduling algorithm for multi-cell deployment is proposed that selects user equipments (UEs) in UL and DL directions. The algorithm assumes fixed transmission power in the UL and the DL. It ignores the interferences among base stations (BSs) and among the UEs. But not taking into account the inter-BS interference does not give insight into real deployment scenarios. In [12], a FD multi-cell system has been analyzed employing UE selection and fixed UL and DL transmission powers. They have proposed to handle interference among BSs by null forming in the elevation angle of the BS antennas. A user selection algorithm for a FD system was proposed in [13] where total cancellation of interference among BSs were assumed. While it would be ideal to totally cancel inter-BS interference, in practice, it is not possible to

have perfect inter-BS interference cancellation. Goyal *et al.* [14] present a FD multi-cell system assuming full cancellation of SI. But expecting full cancellation of SI is way beyond the current state of the art which can provide a SI cancellation of 110 dB.

The aforementioned works give interesting insights on FD multi-cell system performance. But the inference drawn from them does not properly reflect the practical FD deployment scenario due to various simplified assumptions regarding SI and inter-BS interference. Interference dynamics of FD multi-tier cellular networks are also not captured from such simplified models. In this regard, in this paper, we take a more practical approach to analyze FD multi-cell networks considering all possible interference that might occur in such networks. For this reason, we consider the well accepted dense urban model of Madrid city proposed in METIS project [15] for analyzing a multi-cell, multi-tier FD network that consists of macro and pico BSs. We have identified the critical challenges for real world deployment of multi-cell multi-tier FD networks. We have analyzed the FD performance trade-offs for a dense urban cellular network. We have also proposed user selection and power control algorithms for a cloud-based radio access network (C-RAN) deployment of a FD network that is able to provide significant performance gain.

The rest of the paper is organized as follows: in Section II, a FD multi-cell network has been discussed and compared with a HD network. A user selection algorithm has been proposed in Section III. Investigated system model and simulation results have been presented in Section IV. Finally, concluding remarks are made in Section V.

II. FD MULTI-CELL DEPLOYMENT

The interference pattern in a multi-cell scenario for a HD and a FD deployment are shown in Fig. 1. In a HD implementation, the transmission in the UL and the DL are aligned. All the neighboring BSs transmit in the DL at the same subframe and receive transmissions from their connected users in the UL at the same subframe. Hence, the possible sources of interference are: UL-to-UL interference and DL-to-DL interference. This is illustrated in Fig. 1a where UE11 and UE12 are connected to BS1 and UE21 and UE22 are connected to BS2. During the DL transmission, BS1 transmits to UE12 and causes interference I_{DD} to the UE22. Similarly, in the UL transmission subframe, the cell edge user UE21 sends its signal to BS2 and in doing so, it creates interfering signal I_{UU} to the uplink transmission of the neighboring cell user UE11.

The interference scenario becomes much more complicated for the FD system. The possible source of interference in a FD multi-cell deployment are (cf. Fig. 1b):

- SI between the Tx and Rx chain of a BS, I_{SI} ;
- Inter-cell UL-to-UL interference I_{UU} ;
- Inter-cell and intra-cell UL-to-DL interference I_{UD} ;
- DL-to-UL interference I_{DU} among neighboring BSs;
- Inter-cell DL-to-DL interference I_{DD} .

Here, we can see that both BSs generate SI, I_{SI} between their Tx and Rx chains. BS1 generates DL-to-DL interference, I_{DD} to UE22 and DL-to-UL interference, I_{DU} to BS2. UE21 generates inter-cell UL-to-UL interference, I_{UU} to the UL transmission of UE11. It also generates intra-cell and inter-cell UL-to-DL interferences I_{UD2} and I_{UD1} to UE22 and UE12, respectively. Hence, it can be seen that a complex array of interference occurs in a multi-cell FD deployment and cancelling only the SI is not enough to harvest the promising gain of a FD system [16]. This will be evident in our analysis and obtained results in the subsequent sections.

III. USER SELECTION AND POWER CONTROL

The throughput gain in a FD system depends on different network parameters, e.g., distance among BSs, user distribution, mobility, channel propagation condition, DL & UL transmission power levels, etc. For this reason, a FD system should work opportunistically, i.e., when the network condition is favorable, a BS should operate in FD mode and in case of an unfavorable condition, the BS should switch back to HD mode. Hence, the operating mode of the FD system can be attributed a hybrid FD mode rather than a pure FD mode. In our analysis, the BSs are assumed to be FD capable while the user equipment (UE) operates in HD mode.

In this paper, we have used a proportional fair centralized scheduler that maximize the sum log throughput of the scheduled users at any given time slot. The scheduler employs a proportional fair schedule and pair mechanism for scheduling users. First, it randomly selects a user, then it schedules a second user such that the sum log throughput of the users' rate is higher than that of the single user in the previous scheduling step. In a similar fashion, it continues to schedule the next user and so on until the sum log throughput of users' rate is higher than the previous schedule. The scheduler objective function can be defined as

$$\max \left(\sum_{n=1}^N \sum_{u=1}^{U_n} [\log(R_{n,u}^{DL})(t) + \log(R_{n,u}^{UL})(t)] \right) \quad (1)$$

$$\text{s.t. } \begin{cases} P_{n,u}^{DL}(t) = P_n^{DL,max}, \text{ when a BS has user} \\ P_{n,u}^{DL}(t) = 0, \text{ when a BS has no user} \\ P_{u,n}^{UL}(t) = P_u^{UL,max}, \text{ when a user is scheduled} \\ P_{u,n}^{UL}(t) = 0, \text{ when a user is not scheduled} \\ R_{n,u}^{DL}(t) \times R_{n,u}^{UL}(t) = 0, n = \{1, 2, \dots, N\} \end{cases} \quad (2)$$

where N is the number of BSs, U_n is the number of scheduled users in serving cell (i.e., BS) n , $R_{n,u}^{DL}(t)$ and $R_{n,u}^{UL}(t)$ are the average DL and UL data rates, respectively, for user u at the serving cell n at time slot t and $1 \leq u \leq U_n$. The first four constraints enforce power control scheme for BSs and UEs. A binary power control scheme has been employed where a BS is active (and transmits at full power $P_n^{DL,max}$) if it has any user connected to it otherwise it is switched off. Similarly, if a UE is scheduled at a certain time period it transmits at full power $P_u^{UL,max}$ otherwise it is switched off. The fifth

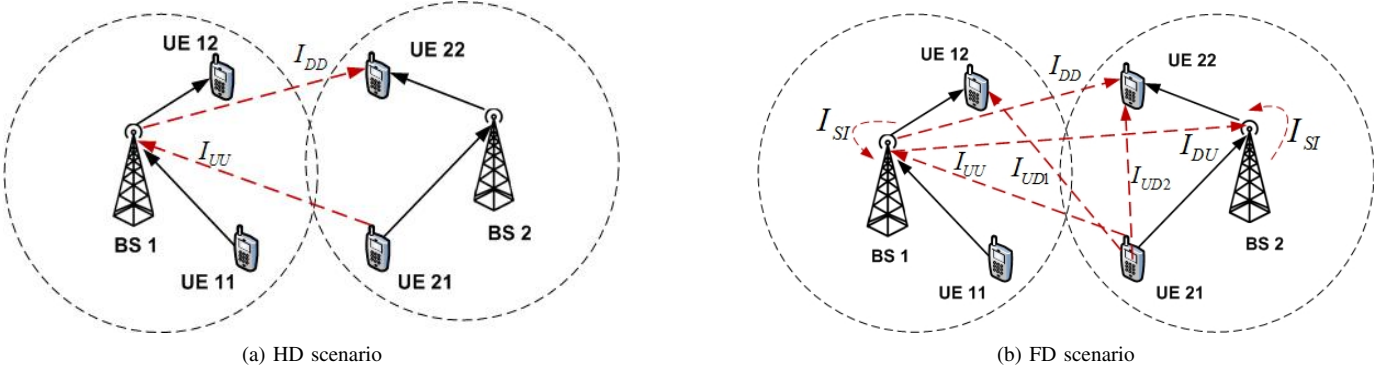


Fig. 1: HD and FD multi-cell scenarios

constraint enforces the half-duplex mode of operation for the UEs, i.e., at any given time slot t , they can either transmit to the BS they are attached to or receive transmission from the BS but not do the both simultaneously.

The instantaneous DL rate of a user can be expressed as

$$\begin{aligned} R_{n,u}^{DL}(t) &= \log_2 \left(1 + SNIR_{n,u}^{DL}(t) \right) \\ &= \log_2 \left(1 + \frac{P_{n,u}^{DL}(t) H_{n,u}^{DL}(t)}{\sigma^2 + P_I^{DL} + P_I^{UL}} \right) \end{aligned} \quad (3)$$

where the nominator of the signal to noise and interference ratio (SNIR), $SNIR_{n,u}^{DL}(t)$ consists of the DL transmission power of the BS n , $P_{n,u}^{DL}(t)$ and the DL channel gain $H_{n,u}^{DL}(t)$ between the BS n and the DL user u ; the denominator composes of the noise power σ^2 , inter-cell interference from the neighboring BSs, P_I^{DL} and the interference from the other users, P_I^{UL} .

Similarly, the instantaneous UL rate of a user can be expressed as

$$\begin{aligned} R_{n,u}^{UL}(t) &= \log_2 \left(1 + SNIR_{n,u}^{UL}(t) \right) \\ &= \log_2 \left(1 + \frac{P_{n,u}^{UL}(t) H_{n,u}^{UL}(t)}{\sigma^2 + P_n^{DL}(t) \times g + P_I^{DL} + P_I^{UL}} \right) \end{aligned} \quad (4)$$

where the nominator of the SNIR, $SNIR_{n,u}^{UL}(t)$ consists of the UL transmission power of the users and the channel gain between the user u and the BS n . In the denominator, the first term is the noise power, the second term is the self interference, i.e., the product of the BS's DL power and the self interference cancellation (SIC) gain g , the third term is the inter-BS interference among the neighboring BSs and the last term is the UL interference power from the neighboring users.

The goal of the centralized scheduler is to select UEs in the UL and the DL directions in a way such that the utility in equation (1) is maximized. First, it schedules a user (either in UL or in DL) that has the highest utility value. Then it tries to schedule another user such that the achieved utility is larger than it was in the previous step when the first user was scheduled. And it continues to schedule more users until the

achieved system utility increases than that at the previous step. The scheduler stops to schedule users once the system utility decreases after scheduling a new user.

A. Selecting users

Selection of users for transmission is done in an optimal manner such that it maximizes the system performance. In the HD case, as the DL transmission nodes (i.e., the BSs) have known locations, it is possible to accurately compute the interference from neighboring BSs. Hence, it is convenient to estimate the channel gains with respect to the neighboring BSs for each DL UE. And this does not require the information regarding the scheduling decision of the neighboring BSs. For this reason, it is possible to make an optimal UE selection decision in the DL. On the contrary, for the UL scheduling case, it is not possible to calculate interference from the neighboring cells unless the scheduling decisions of the cells are available. For the FD case, as the DL and UL take place simultaneously it is not possible to optimally compute the channel gains in either directions without complete scheduling information of the neighboring BSs. This will generate more backhaul traffic than the HD deployment. We have implemented a centralized scheduler that has global channel state information. The scheduling algorithm is described in the following subsection.

B. Centralized Scheduling

In a C-RAN case, a centralized scheduler can have a global view of the system i.e., it has information about the user distribution, BS power levels, channel information, etc. Thus this centralized scheduler is able to schedule users intelligently to favor FD modes for the BSs which will increase the overall system throughput. Algorithm 1 shows the steps followed in the user selection process by a centralized scheduler. In each scheduling epoch, the vector B contains all the active BSs in the network, the vector W is the weight vector having the size of the number of active users which is initialized to 1. A matrix ϕ is used that will contain the IDs of the scheduled users in different scheduling epoch. The scheduler schedules a user either in the UL or in the DL direction depending on the weighted sum rate maximization of the scheduled users.

Algorithm 1 User Selection: Centralized Scheduling

```

1:  $B \leftarrow \{1, 2, 3, \dots, N_B\}$ 
2:  $W \leftarrow 1$ , weight vector initialized to 1
3:  $\mu \leftarrow \text{constant}$ 
4:  $\nu \leftarrow \text{constant}$ 
5:  $\phi \leftarrow \{\phi(t_1), \phi(t_2), \dots, \phi(t_T)\}$ 
6:  $M_{max} \leftarrow 0$ 
7: while  $W > \mu$  do
8:   for  $b \leftarrow B(1)$  to  $B(N_B)$  do
9:     for  $p \leftarrow \{u, d\}$  do
10:      for  $k \leftarrow 1$  to  $K_p$  do
11:         $M(k) \leftarrow GetMetric(k, W)$ 
12:         $\{\phi(i), M(b)\} \leftarrow \{\arg \max_{d \in \{u, d\}} M\}$ 
13:        if  $M(b) \leq M_{max}$  then
14:          break
15:        if  $M(b) > M_{max}$  then
16:           $M_{max} \leftarrow M(b)$ 
17:           $\phi(t_i) \leftarrow \phi_k(i)$ 
18:           $W(k) \leftarrow W(k)/\nu$ , update the weight so that the
   user is not scheduled in the next iteration

```

The weight vector W is updated in a way that make sure all the active users are scheduled either in the UL or in the DL direction (Line 7). For each BS, the algorithm finds a DL/UL user (say $\phi(i)$) that has the highest metric calculated by $GetMetric()$ (Line 11). The $GetMetric()$ algorithm that calculates the weighted sum throughput of the scheduled users is not presented in this paper due to space limitations. In the very first iteration the selected user is the first scheduled user, hence, its metric is assigned as the maximum metric (Line 16). Then the user is added in the scheduled user list and its associated weight is updated such that in the next scheduling iteration it is not selected again (Line 17 and Line 18). In the next iteration, the scheduler runs through all the BSs, and for each unscheduled user, it calculate the metric for that user and the user scheduled in the previous scheduling epoch. If the new metric ($M(b)$) is higher than the highest metric in the last run (M_{max}), the new user is selected and included in the schedule list $\phi(t_i)$. The corresponding weight of the newly selected user is updated (Line 16 to Line 18) and the whole process runs again until all the users are scheduled. This gives a bunch of schedules of users where all the users are scheduled at least once. An optimization is then run for the schedules that determines the final user scheduling list based on sum log throughput maximization.

IV. PERFORMANCE ANALYSIS

We have used the Madrid grid model proposed in the METIS project [15] for the dense urban FD cellular network deployment evaluation. The Madrid grid model is shown in Fig. 2 [15]. The building layout of the grid can be seen in Fig. 2a. It consists of buildings (with entrances) that have different dimensions and heights, roads, bus stops, park, side walk and crossing lanes. This model captures the typical propagation environment of a modern city. Fig. 2b shows the layout of the

TABLE I: Simulation parameters for Madrid grid model

Parameter	Value	Unit
Sector/Macro	3	-
Number of Picos/Macro BS	12	-
Maximum Macro BS power	43	dBm
Maximum Pico BS power	24	dBm
Maximum UE power	23	dBm
Thermal noise density	-174	dBm/Hz
Transmission mode	SISO	-

buildings with BS placements. In this model each macro BS has three sectors and there are 12 pico BSs per macro BS. The red arrow shows the locations of the macro antennas and the orange dots represents the pico BS locations. The simulation parameters for the Madrid grid model is listed in Table I. The propagation model for the Madrid grid considers channels between BS to UE, BS to BS as well as the UE to UE. The model also considers outdoor-to-indoor and indoor-to-outdoor propagation. A fully indoor propagation model for indoor UE-to-UE channel has been considered. In the simulation, UEs were dropped in the considered simulation area on an average 10 UEs/BS. The UEs connect to a BS depending on the maximum received signal strength. The UEs were then scheduled for transmission by the scheduler.

For the considered centralized scheduling case, the scheduler selected users belonging to the active cells (i.e., the BSs that have connected users) based on their achievable data rate. For the HD case, one user per active cell is selected. For the FD case, for each active cell, the scheduler schedules a user for transmission either in the UL or in the DL. Based on algorithm 1 it schedules another user in the opposite direction. It should be noted that, if the inclusion of a user is not favorable to the resulting system performance, the scheduler might schedule only one user either in the UL or in the DL or it might not schedule any user at all for that BS for a particular scheduling epoch. Hence, some of the FD BSs might fall back to the default HD operating mode. To investigate the impact of SIC in FD system performance, a range of SIC value is used. Three different interference cancellation modes have been studied: a) the case when only SI is canceled by SIC value, b) the case when in addition to the SIC an inter-BS interference cancellation (*IBIC*) similar to the SIC is employed and c) the case when a SIC and a fixed *IBIC* of 30 dB is used. In the following subsections the impact of SIC and *IBIC* on achievable user rate and network fairness are discussed.

A. User rate vs. SIC

Fig. 4 shows the geometric mean of user rate against various SIC values for different interference cancellation schemes. It can be seen that FD system has much better performance than the TDD. When only SIC is applied (the green solid line), the system performance is unaffected up until SIC = 82 dB, after which it increases gradually with increasing SIC and saturates when SIC = 160 dB. This shows that increasing the SIC after a certain threshold value does not provide much performance gain. In fact, when only SIC is applied, after SIC = 140 dB no significant performance improvement is observed.

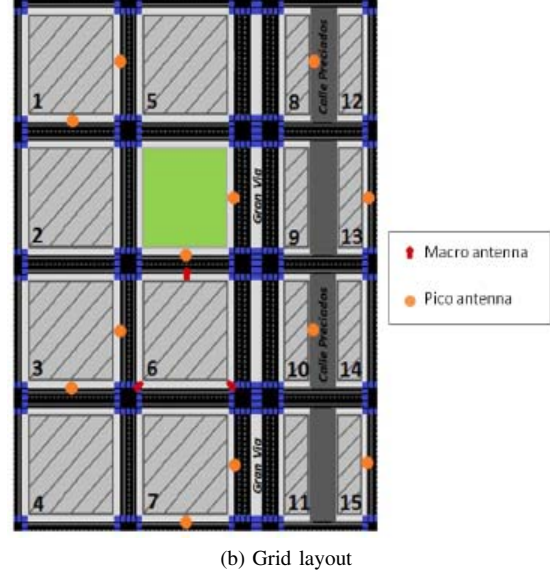
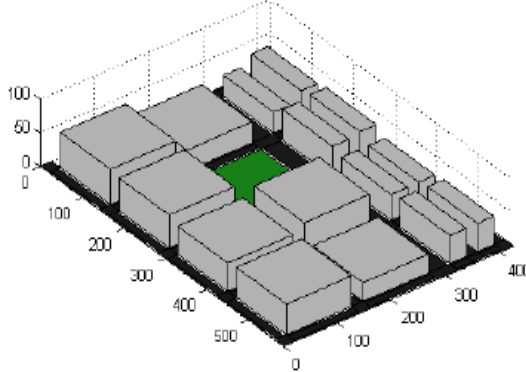


Fig. 2: Madrid grid model layout

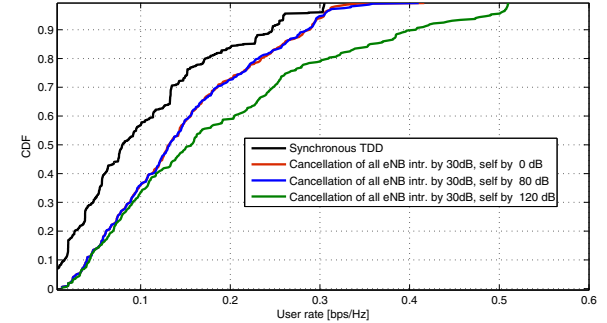
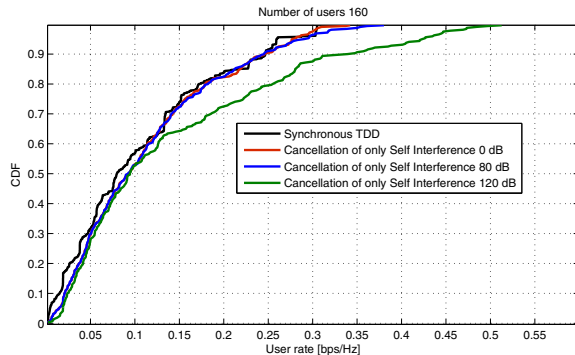


Fig. 3: Madrid grid model: CDF of user rate

It is interesting to note that applying a constant *IBIC* of 30 dB (the red solid line) gives a significant performance boost of almost 50%. We have used *IBIC* = 30 dB because this amount of interference cancellation is achievable in the digital domain. Again until the *SIC* = 82 dB, the system performance remains constant after which it starts to increase and saturates at around 160 dB. Now, to observe the impact of *IBIC*, the interference among BSs is canceled by the same amount as the *SIC* (the solid blue line). It is interesting to note that, for lower *SIC*, the system performance increases almost linearly with the *IBIC* until *IBIC* = 48 dB, after that the performance gain is independent of the *IBIC* and it picks up again after *SIC* = 80 dB with increase in the *SIC* and saturates at *SIC* = 160 dB. This shows that, *IBIC* is very significant for performance improvement in a centralized (i.e., a C-RAN based) FD system and applying a constant *IBIC* (e.g., 30 dB) is sufficient to achieve a considerable performance gain.

Fig. 3a shows the CDF of user rate when only *SIC* is applied. Three different *SIC* values (0, 80 and 120 dB) are used. It can be observed that an *SIC* = 80 dB does not give much performance gain when compared to a *SIC* = 0 dB. A gain in user rate is observed when *SIC* = 120 dB, this shows that a certain threshold of *SIC* is required to achieve FD gain. Fig. 3b shows the CDF of user rate when an *IBIC* of 30 dB is applied in addition to the *SIC*. It is clear from the figure that the *IBIC* increases the performance by a considerable margin. The *IBIC* boosts the system performance for higher *SIC* values. A 44% gain in user rate can be achieved for 70% of the users when an *SIC* = 120 dB and *IBIC* = 30 dB is applied compared to the case when only *SIC* = 120 dB is applied.

B. System throughput (ST) vs. fairness

Fig. 5 shows the ST vs. Jain's fairness index (JFI) performance. It can be seen that the FD baseline (i.e., when *SIC* = 0

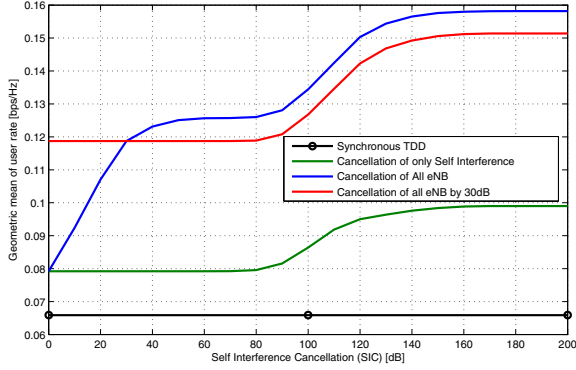


Fig. 4: Madrid grid model: user rate vs. SIC for HD and FD systems

TABLE II: Madrid grid: JFI vs. sum throughput

System	Centralized scheduling	
	JFI	ST [bps/Hz]
TDD	0.6024	33.9828
FD (SIC only)	0	0.6374
	80	0.6286
	120	0.5700
FD (SIC + IBIC = 30 dB)	0	0.7312
	80	0.7293
	120	0.6619
		61.4693

dB and $IBIC = 0$ dB) has 6% throughput gain over the TDD. Applying a $IBIC = 30$ dB increases the throughput gain by 31.5% while increasing the JFI by a considerable amount. It is to be noted that increasing the SIC to 80 dB does not provide any significant throughput gain. But increasing the SIC to 120 dB provides a further throughput gain of 29.5% with a slight increase in JFI. The FD system with SIC = 120 dB and $IBIC = 30$ dB provides a ST gain of 81% over the TDD.

V. CONCLUSION

In this paper, FD deployment in a dense-urban multi-cell environment has been investigated. For a dense-urban scenario, the deployment model of Madrid-grid proposed in the METIS [15] project has been considered. Algorithms for user selection

and power control have been proposed. The results obtained through extensive system-level simulations suggest that for successful deployment of a FD cellular network, BSs need to be aware of the scheduling and power setup decisions of their neighboring BSs. Also, in addition to mitigating SI, minimization of inter-BS interference is critically important for FD cellular systems. For the investigated FD C-RAN model, it has been found out that only employing a $SIC = 120$ dB gives a throughput gain of 28% whereas adding an additional 30 dB $IBIC$ can give a throughput gain of 81%. The additional critical challenges that need to be addressed are interference mitigation among UEs and minimizing the backhaul control traffic. Investigation of these issues are the subject of our on going research.

ACKNOWLEDGMENT

We would like to thank Huan Wu and Eddy Hum of Huawei Canada Research Center for their expert opinion and valuable discussions.

REFERENCES

- [1] Cisco, "Cisco visual networking index: Forecast and methodology 2013-2018," *Cisco White Paper*, 2014.
- [2] S. Hong, J. Brand, J. I. Choi, M. Jain, J. Mehlman, S. Katti, and P. Levis, "Applications of self-interference cancellation in 5g and beyond," *IEEE Communicatoin Magazine*, vol. 52, pp. 114–121, Feb. 2014.
- [3] J. I. Choi, M. Jain, K. Srinivasan, P. Levis, and S. Katti, "Achieving single channel, full duplex wireless communication," in *Proc. of the MobiCom*, Sept. 2010.
- [4] A. K. Khandani, "Methods for spatial multiplexing of wireless two-way channels," *US Patent No. 7,817,641*, Oct. 2010.
- [5] M. E. Knox, "Single antenna full duplex communications using a common carrier," in *Proc. of the 13th Annual Wireless and Microwave Tech. Conf.*, Apr. 2012.
- [6] D. Bharadia, E. Mcmillin, and S. Katti, "Full duplex radios," in *Proc. of the ACM SIGCOMM*, Aug. 2013.
- [7] M. Duarte and et al., "Design and characterization of a full duplex multi-antenna system of wifi networks," *IEEE Trans. Vehic. Tech.*, vol. 63, pp. 1160–1177, Mar. 2014.
- [8] Huawei, "Full duplex technology for 5g," *Huawei Innovation Research Program Journal*, pp. 62–69, Jan. 2015.
- [9] DUPLO, "The EU 7th project full-duplex radios for local access (duplo)," Available at <http://www.fp7-duplo.eu/>.
- [10] D. Nguyen, L.-N. Tran, P. Pirinen, and M. Latva-aho, "On the spectral efficiency of full-duplex small cell wireless systems," *arXiv:1407.2628 [cs.IT]*, July 2014.
- [11] X. Shen, X. Cheng, L. Yang, M. Ma, and B. Jiao, "On the design of the scheduling algorithm for the full duplexing wireless cellular network," in *Proc. of the IEEE GLOBECOM*, Dec. 2013.
- [12] Y.-S. Choi and H. Shirani-Mehr, "Simultaneous transmission and reception: algorithm, design and system level performance," *IEEE Transaction on Wireless Communication*, vol. 12, pp. 5992–6010, Dec. 2013.
- [13] H.H.Chi, "On the design of user pairing algorithms in full duplexing wireless cellular networks," in *Proc. of the International conference on Information and Communication Technology Convergence (ICTC)*, Oct. 2014.
- [14] S. Goyal, P. Liu, S. Hua, and S. Panwar, "Analyzing a full duplex cellular system," in *Proc. of the 44th Annual Conference on Information Science and Systems (CISS)*, Mar. 2013.
- [15] P. A. et al., "Mobile and wireless communications enablers for the twenty-twenty information society (metis)," *Seventh Framework Program, Deliverable D6.1*, Oct. 2013.
- [16] A. Sabharwal, P. Schniter, D. Guo, D. W. Bliss, S. Rangarajan, and R. Wichman, "In-band full-duplex wireless: Challenges and opportunities," *IEEE Journal on Sel. Area in Comm.*, vol. 32, pp. 1637–1652, Sept. 2014.

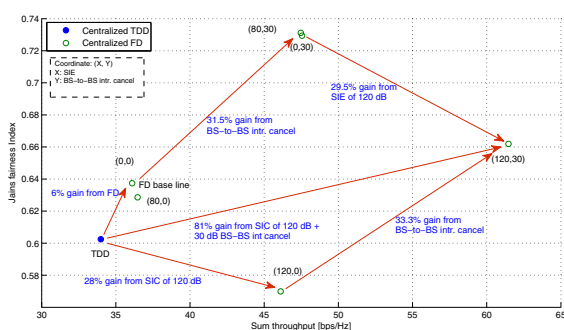


Fig. 5: Madrid grid model: centralized scheduling sum throughput vs JFI